Charge transfer in hyperthermal energy collisions of Li^+ with alkali-metal-covered Cu(001). I. Dynamics of charge state formation

E. R. Behringer,* D. R. Andersson,† and B. H. Cooper
Laboratory of Atomic and Solid State Physics, Cornell University, Ithaca, New York 14853-2501

J. B. Marston
Department of Physics, Box 1843, Brown University, Providence, Rhode Island 02912
(Received 25 April 1996; revised manuscript received 24 July 1996)

We have measured the charge state fractions in the scattered flux versus the work-function change induced by Cs adsorbates when hyperthermal energy Li^+ ions are incident on Cs/Cu(001). As the work function ϕ decreases from its clean surface value ($\phi = 4.59$ eV), the positive ion fraction decreases from 0.64 to less than a few percent, while the negative ion fraction slowly increases from less than a few percent to 0.14 at the lowest work function attained ($\phi = 1.29$ eV). Theoretical calculations based on a many-body solution to the time-dependent, multiple-state, Anderson-Newns model of resonant charge transfer qualitatively reproduce the observed trends. Detailed examination of the calculations shows that the theoretically predicted dependence of the final charge state fractions on work function and the dynamics of the charge-transfer process are both strongly influenced by the wave function of the ion-surface system when the incident ion is close to the surface and also by the changing relationships between the relevant time and energy scales as the scattered particle moves away from the surface. [S0163-1829(96)08144-1]

I. INTRODUCTION

The study of charge transfer in ion-surface collisions has intensified over the last decade,[1–3] in part because charge transfer plays a fundamental role in dynamical processes such as molecular chemisorption and dissociation, and because charge transfer can be used to probe the ion-surface interaction. In addition, charge transfer plays a role in applications such as secondary-ion-mass spectroscopy and reactive ion etching.[4] Significant experimental and theoretical progress has therefore been made in an effort to obtain an increasingly detailed understanding of charge transfer.

Despite this progress, understanding the rich complexity of the charge-transfer process demands more precise measurements of branching ratios to different final states. This presents an experimental challenge, since many outcomes are possible when a positively charged ion collides with a surface. One of these is simply that the ion scatters as a positive ion — that is, without a change of its initial charge state. Numerous alternative outcomes are made possible by electron transfer between the scattering ion and the surface, which allows the charge state of the ion to change. For example, the ion may be neutralized into the ground state or into an excited state, or may even form a negative ion. The charge state of the scattering ion can be changed by different charge-transfer mechanisms, including resonant, Auger, and direct radiative mechanisms. To develop an understanding of the different mechanisms, knowledge of the branching ratios to the different possible charge states and their dependence on experimentally controlled variables (e.g., velocity, work function) is required. Subsequent comparison of theoretical predictions to measured charge state fractions may then provide insight to the dynamics of charge transfer, which is the fundamental goal of this research.

In this paper and the following companion paper (which we refer to as paper II) we will present measurements of branching ratios for collisions of Li^+ ions with clean and alkali adsorbate-covered Cu(001) surfaces,[5,6] and examine the dynamics of charge transfer predicted by a many-body solution to the time-dependent, multiple-state, Anderson-Newns model of resonant charge transfer.[7] Here we concentrate on the resonant mechanism of charge transfer because it is thought to dominate for alkali ion-surface systems,[2] and we ignore the Auger and direct radiative mechanisms since the probability for scattering into final states via these mechanisms is thought to be small.[8] Also, we only model the outgoing trajectory of the scattered particles since experiments have shown that, for particles which are described by relatively simple trajectories, the outgoing trajectory determines the final charge state.[9,10] We find that the present theory qualitatively reproduces nearly all the trends seen in the data.

Early experiments concentrated on the scattering of low-energy alkali ions from clean metal surfaces, and showed that the dominant charge states in the scattered flux are the positively charged states and the neutral states.[11] The results of these experiments could be described well with the single-state Anderson-Newns model of resonant charge transfer.[12–14] Later experiments[15] utilizing low and hyperthermal energy ions could also be well described with this model when using atomic state lifetimes and energies that had since been calculated by Nordlander and Tully.[16–18] The same model, when modified to include the effect of the ion velocity parallel to the surface plane,[19–23] can be used to describe experiments which utilize grazing scattering geometries.

Scattering experiments with low work-function surfaces have shown that other final charge states, such as the negative ion state and neutral excited states, can be present in the scattered flux.[5,6,24–28] In early work, the formation of negative ions was assumed to be a one-electron process, so that the single-state Anderson-Newns model could be

applied.[24,29,30] This assumption allowed the prediction of the qualitative dependences of the negative ion yield on work function and ion velocity. However, one is forced to apply the model differently at different work function values, which is unsatisfactory. Additionally, the single-state model is simply not capable of describing experiments in which multiple (i.e., more than 2) states are observed in the scattered flux. To describe the experimental observations of multiple states in the scattered flux theoretically, one is therefore compelled to abandon the single-state model in favor of models which include multiple states.

Over the past decade, a number of multiple-state models have been developed.[2,7,31–40] Some of these models have, in addition to the ground positive ion state and the ground neutral atom state, included the negative ion state[31–35] while others include both the negative ion state and a neutral excited state.[36,37,39] The data presented here will be used to test a many-body model of resonant charge transfer,[7] which allows for the production of positive ions, ground state neutral atoms, negative ions, electron-hole pairs, and excited-state neutral atoms.

We point out that an alkali-covered surface has a spatially varying electrostatic potential, and previous work[14,24,29,30,38,40–46] has shown that when this inhomogeneous potential is included in charge-transfer models, the quantitative agreement between the model and experimental data is improved. This is because the scattered projectile will in general explore the full three-dimensional nature of the inhomogeneous potential. Such potentials have been calculated theoretically,[48,49] and spatially varying potentials have been used with the single-state Anderson-Newns model to make comparisons to experiment.[40,42] Recently, such a potential has also been incorporated into the many-body model used in this paper to describe the neutralization behavior of Li^+ scattering from alkali-covered Al(001).[46] A result of these previous works is that inclusion of the local electrostatic potential does not qualitatively change the work-function dependence of the charge state fractions predicted by the theory when alkali ions scatter from a surface atom, and in fact the quantitative changes in the neutral fractions are also small. This result suggests that the dynamics are effectively predicted by a model in which the electrostatic potential is treated as uniform along the surface. Since calculations involving the inhomogeneous potential are especially computationally demanding with the many-body model if the experimental situation requires averaging over many different trajectories (as is the case for the experiments discussed here), we do not include it.[47] Instead, we will focus on a number of trends predicted with the model and compare these to the trends seen in the data and then look in detail at the dynamics of the charge transfer predicted by the model. We will discuss the effect of the inhomogeneous potential further in Sec. VI.

In this paper and in paper II, we present a study of charge transfer in systems where hyperthermal energy Li^+ ions collide with clean and alkali adsorbate-covered Cu(001).[5,6] We measured the charge state fractions in the scattered flux using the time-of-flight technique together with a neutral alkali atom detector. Using low-level photon-counting techniques, we also determined the relative probability with which the incident ion will scatter into the $Li^0(2p)$ state by measuring the photon flux due to the $Li^0(2p) \rightarrow Li^0(2s)$ transition. In this paper, we compare theoretical predictions to the measurements of the charge state fractions; in paper II, we discuss the measurements of the relative probability of scattering into the $Li^0(2p)$ state. Here the comparison between theory and experiment reveals important qualitative features (spin, multiple states, inclusion of the adsorbate-induced electrostatic potential) that such a theory must possess, and provides insight into the dynamics of resonant charge transfer. In particular, we will discuss the role of the wave function of the ion-surface system when the ion is close to the surface, of the energies of the atomic states relative to the Fermi level of the metal, and of the lifetimes of the atomic states in the vicinity of the surface in determining the dynamics of resonant charge transfer.

In Sec. II, we describe the experimental techniques used to measure the charge state fractions. In Sec. III, we present the data, followed by a description of the theory in Sec. IV. We compare the theoretical predictions to the data in Sec. V, and also discuss the effect of the local electrostatic potential of the adsorbates used to change the surface work function in Sec. VI. We conclude the paper with a summary in Sec. VII.

II. EXPERIMENTAL TECHNIQUE

Our data were obtained in a versatile, two-tiered, ultrahigh vacuum (UHV) chamber that has been described elsewhere;[50] we provide relevant details here. The upper tier is devoted to preparing and monitoring the sample surface and the lower tier is used for performing the ion-scattering measurements. The upper tier is equipped with a set of reverse-view optics for low-energy electron diffraction (LEED), a set of optics for Auger electron spectroscopy (AES), a Kelvin probe, three alkali getter sources, a sputter gun, and a residual gas analyzer. The lower tier of the chamber contains the final electrostatic lens for focussing the ion beam onto the sample, a hemispherical electrostatic analyzer,[51] and a neutral particle detector (NPD) for alkalis.[52,53]

A. Sample preparation

Before the measurements of the charge state fractions were performed, both the orientation and the condition of the Cu(001) sample were checked using LEED and ion scattering, as described elsewhere.[5] Our crystal cleaning procedure consisted of sputtering the sample with Ar^+ ions with kinetic energies ranging from 0.5 to 1.0 keV, and then heating the sample via electron beam bombardment to at least 600 °C for 1–3 min. Typical currents on sample while sputtering were 1–2 μA. The resulting surface was found to be clean to within the sensitivity of AES.

To change the work function of the sample surface from its initial value ϕ_i to its final value ϕ_f, varying amounts of Cs were deposited on the surface with an outgassed, commercially available getter source.[55] We measured the work-function change $\Delta\phi = \phi_f - \phi_i$ by using a Kelvin probe. To produce overlayers with different alkali coverages, we varied the deposition time and then gently (i.e., without adsorbate desorption) annealed the sample to 200 °C (which we expect enhances surface diffusion, which in turn leads to the spatial

uniformity of the overlayer). This procedure led to highly reproducible changes in the work function as determined by Kelvin probe measurements.

The uniformity and cleanliness of the overlayers were checked with AES. This was done by preparing an overlayer and then acquiring Auger spectra from different locations on the sample. The Auger spectra indicated that the Cs coverage was uniform to within the resolution of AES and that the Cs overlayers were clean. During the measurement of the charge state fractions, the pressure inside the UHV chamber was in the high 10^{-11}-torr range. This corresponds to a monolayer formation time of approximately 20 h if one assumes a sticking coefficient of unity. Thus we expect no significant residual gas adsorption to occur during our data acquisition, which takes less than 1 h when measuring charge state fractions. Spot checks during data acquisition (see below) verify that no significant residual gas adsorption occurs.

Work done by Cousty, Riwan, and Soukiassian on the Cs/Cu(001) surface[56] shows that the Cs overlayers are disordered for coverages up to $\theta=0.37$,[57] where $\theta=1$ corresponds to having one adsorbate atom for every substrate surface atom. Since our heaviest Cs overlayers corresponded to a coverage of $\theta\approx 0.14$,[57] we expect that the Cs overlayers in our experiments are also disordered.

B. Charge state fraction measurements

We used the time-of-flight technique together with a neutral particle detector (NPD) to measure velocity-resolved charge state fractions. The NPD is mounted on a rotating table in the bottom tier of the scattering chamber whose axis of rotation coincides with the axis of the sample manipulator, as determined by an alignment procedure similar to that described by McEachern *et al.*[50] The NPD utilizes surface ionization[52,53] and the procedure for measuring the charge state fractions has been presented in detail elsewhere.[53] Knowing the Li^+ ion beam current, the beam pulse length, and beam chopping frequency, we estimate that the sample is hardly dosed ($\theta=10^{-4}$, where $\theta=1$ corresponds to one alkali adsorbate for every copper surface atom) by the incident beam. We also believe that the alkali overlayers do not change on the time scale of the data acquisition because the measured ion fractions do not change significantly during the compilation of the spectra, except when the ion fractions are a few percent or less. In these latter cases, the experimental uncertainties are somewhat larger.

A typical time-of-arrival spectrum is shown in Fig. 1(a) for the case of 400-eV Li^+ incident on the clean Cu(001) surface, along the $\langle 100\rangle$ azimuth, with $\theta_i=65°$ as measured from the surface normal. The final angle of detection is $\theta_f=64°$, also measured from the surface normal. The solid line shows the signal due to both neutral atoms and ions, i.e., the total flux, while the dashed line shows the signal due to the ions only (which is derived by subtracting the neutral time-of-arrival spectrum from the total time-of-arrival spectrum). The vertical lines in Fig. 1(a) define the time interval over which the intensity is integrated so that the positive ion fraction can be obtained.[54] The raw data have been smoothed for display in this plot (we note that the raw data were used to calculate the neutral fractions and their associated uncertainties). In Fig. 1(b), the same data are shown and the time

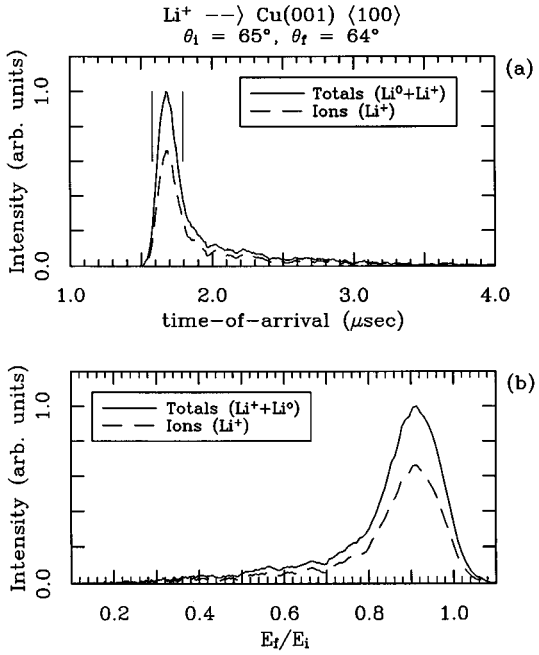

FIG. 1. (a) A typical time-of-arrival spectrum, for the case of 400-eV Li^+ ions incident on clean Cu(001), $\theta_i=65°$. The final angle of detection was $\theta_f=64°$. The angles are measured with respect to the surface normal. Solid line: ions plus neutral atoms. Dashed line: ions only. The vertical lines indicated the interval over which the spectra are integrated in order to obtain the ion fractions. (b) The corresponding energy spectrum. Solid line: ions plus neutral atoms. Dashed line: ions only.

axis has been converted to reduced energy, E_f/E_i, where $E_i=400$ eV is the incident energy of the Li^+ ion beam, and E_f is the final energy after scattering.

III. DATA

We have measured the work function dependence of the charge state fractions that results when 400-eV Li^+ ions impinge on Cs/Cu(001) with an incident angle of 65° and along the $\langle 100\rangle$ azimuth. The final angle of detection is 64°. In Fig. 2, we plot the charge state fractions versus the work-function change $\Delta\phi$ induced by the deposition of Cs on the surface. When the surface is clean, the only charge states in the scattered flux are the positive ion state and the neutral state; no negative ions are present in the scattered flux to within the experimental uncertainty of a few percent (absolute). We know this by comparing the results of two charge state fraction measurements: one in which only the positive ions are rejected, and one in which both positive and negative ions are rejected. The results of these two measurements are the same to within the experimental uncertainty. We note that the error bars in Fig. 2 represent the uncertainty in counting statistics only; the scatter in the data provides a useful measure of the overall uncertainty. As $\Delta\phi$ decreases from zero (i.e., the work function decreases), the positive ion fraction P^+ decreases. For $\Delta\phi>-1.8$ eV, the negative ion fraction is less than a few percent. The negative ion fraction becomes appreciable only for $\Delta\phi<-1.8$ eV, with a maximum value of 0.14 at $\Delta\phi=-3.3$ eV. In the interval of $\Delta\phi$ values where

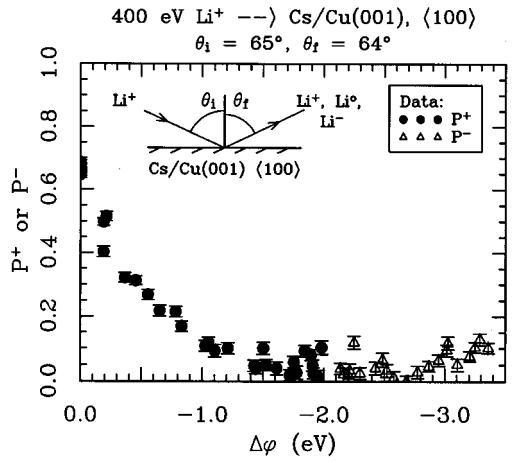

FIG. 2. Measured absolute charge state fractions vs $\Delta\phi=\phi_f-\phi_i$ for 400 eV Li^+ incident on Cs/Cu(001), $\theta_i=65°$, and $\theta_f=64°$. The error bars represent uncertainty from counting statistics only. See text for details.

the negative ion fraction is appreciable, the positive ion fraction does not exceed a few percent.

IV. THEORY

A. One-electron picture

The one-electron picture of electron transfer between an atom and a surface was put forward by Gurney in 1935,[58] and continues to prove useful as a pedagogical tool.[1,59–61,42,62] This picture is useful for understanding how the charge state fractions qualitatively depend on surface work function and ion velocity. We include a brief discussion of the one-electron picture, since its concepts provide a starting point from which to discuss the charge-transfer dynamics predicted by the theory of Marston *et al.* described in Sec. IV B.

We begin by presenting a plot in Fig. 3 of a set of atomic state resonances, within the one-electron picture, for a lithium atom in the vicinity of the Cu(001) surface. These correspond to states of the isolated atom which are shown at the right side of the figure. The energy of each resonance is

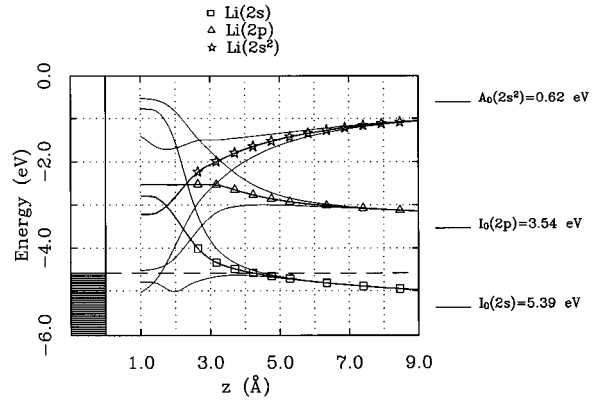

FIG. 3. Li resonance energies, using spline fits to the energies calculated by Nordlander. The corresponding widths are indicated by pairs of thin solid lines.

indicated by a thick solid line drawn through symbols, and the width of each resonance is indicated by a pair of thin solid lines. Increasing resonance widths imply increasing couplings between the atomic states and the levels of the metal, and corresponding increases in transition rates.

The qualitative work function dependence of the various charge state fractions can be deduced by considering the relative energies of the atomic state resonances in Fig. 3. For the clean surface, the $Li^-(2s^2)$ resonance and the $Li^0(2p)$ resonance lie above the Fermi level, and hence we would expect that particles in these states are rarely found in the scattered flux. However, as the work function decreases, the $Li^0(2p)$ resonance becomes degenerate with the occupied levels of the metal and becomes increasingly filled. As the work function decreases further, the $Li^-(2s^2)$ resonance will similarly begin to fill.[63] On the basis of these energetic considerations, it is therefore expected that increasing numbers of $Li^0(2p)$ atoms and negative ions are produced as the work function decreases. These expectations are partially fulfilled since the negative ion yield increases as the work function decreases. However, the yield of $Li^0(2p)$ atoms does *not* steadily increase.[5,6,26–28] The latter point suggests that one must consider more than the energetics in the one-electron picture.

Another important component of this picture is the lifetime broadening of the atomic states, which arises from the interaction between the levels of the metal and the atomic states. As the atom approaches the surface, its states broaden into resonances which have lifetimes inversely proportional to the broadening. When considering a single atomic state interacting with a continuum of occupied metal levels in the adiabatic limit, the occupancy of the atomic state is given by the fraction of the resonance lying below the Fermi level. When the atom has a finite velocity, however, it becomes important to consider the relationship between the relevant time scales; in particular, the time scale set by the resonance lifetime, τ_r, and the time scale set by the velocity of the atom, τ_{motion}. The resonance lifetime decreases rapidly (essentially exponentially) as the atom moves away from the surface, while the velocity of the atom is essentially unchanged after the atom makes its hard collision with the surface. Therefore, as the atom leaves the surface, the relationship between the time scales changes: close to the surface, where $\tau_r \ll \tau_{\text{motion}}$, the atom loses ''memory'' (i.e., the charge state of the atom is independent) of its charge state before its collision with the surface; far from the surface, where $\tau_r \gg \tau_{\text{motion}}$, the charge state of the atom no longer changes; and, at intermediate ion-surface separations, where $\tau_r \sim \tau_{\text{motion}}$, we can expect rapid changes in the charge state of the atom.

Although it is difficult to predict just how the changing relationship between the time scales affects the charge state fractions, it is possible to draw a few conclusions for the case in which *only one* state [e.g., $Li^0(2s)$] is considered, the others [e.g., $Li^0(2p)$ and $Li^-(2s^2)$] being absent. For instance, for sufficiently high velocity, the system will not have time to respond, and the final occupancy of the atomic state will simply be what it was at the distance of closest approach. For sufficiently low velocity, as the atom leaves the surface, the occupancy will follow the fraction of the resonance lying below the Fermi level.[13] We therefore ex-

pect that as the velocity decreases, the distance at which the final occupancy is ''determined'' increases; this implies that the occupancy (i.e., the neutral fraction) will increase as the velocity decreases since the fraction of the $Li^0(2s)$ resonance below the Fermi level increases with distance. Also, as the work function decreases, a larger fraction of the resonance will lie below the Fermi level (at all distances), and so the occupancy should increase as the work function decreases.

B. Theory of Marston *et al.*

To interpret the data presented in section III in detail, we use the theory of Marston *et al.*.[7] This theory is an extension of a version of the time-dependent Anderson-Newns model that was developed in 1985 by Brako and Newns.[64] Here, the model Hamiltonian is[7]

$$\begin{aligned} H(t)=&\sum_{a,\alpha}\left[\epsilon_a^{(1)}(t)P_1+\epsilon_a^{(2)}(t)P_2\right]c_a^{\dagger\alpha}c_{a\alpha} \\ &+\sum_{k,\alpha}\epsilon_k\, c_k^{\dagger\alpha}c_{k\alpha}+\left(\frac{1}{N}\right)^{1/2}\sum_{a,k,\alpha}\left(\left[V_{a;k}^{(1)}(t)P_1\right.\right. \\ &\left.\left.+V_{a;k}^{(2)}(t)P_2\right]c_a^{\dagger\alpha}c_{k\alpha}+\text{H.c.}\right) \\ &+\sum_{a>b}U_{ab}\,n_a\,n_b+\tfrac{1}{2}\sum_a U_{aa}\,n_a(n_a-1). \end{aligned} \tag{1}$$

The first term describes the atomic states, where $\epsilon_a^{(1)}$ ($\epsilon_a^{(2)}$) is the energy of the atomic state a when it is singly (doubly) occupied. The operators $c_a^{\dagger\alpha}$ and $c_{a\alpha}$, respectively, create and annihilate an electron in the atomic state a with spin α. These operators obey the commutation relations $\{c_a^{\dagger\alpha},c_{a'\alpha'}\}=\delta_{aa'}\delta_{\alpha\alpha'}$, where δ is the Kronecker delta function. The c operators are used to define corresponding number operators: $n_a=\Sigma_\alpha c_a^{\dagger\alpha}c_{a\alpha}$. The operators P_1 and P_2 are used to project, respectively, onto states corresponding to a singly or doubly occupied atomic level; we assume them to be self-adjoint. The atomic state index a for lithium is as follows: $a=0$ corresponds to the $2s$ orbital, $a=1$ corresponds to the $2p_z$ orbital, etc. The sum over the spin index α runs from 1 to N, where N is the spin degeneracy ($N=2$ for electrons); this is true for all the sums over α that appear in the Hamiltonian (1).

The second term describes the metal levels, where ϵ_k is the energy of the metal level denoted by momentum k and the operators $c_k^{\dagger\alpha}$ and $c_{k\alpha}$, respectively, create and annihilate an electron of momentum k and spin α. They obey the commutation relation $\{c_k^{\dagger\alpha},c_{k'\alpha'}\}=\delta_{kk'}\delta_{\alpha\alpha'}$, and define the number operator $n_k=\Sigma_\alpha c_k^{\dagger\alpha}c_{k\alpha}$. In reality, k is a three vector, but it can be regarded as a scalar by absorbing the three-dimensional aspects of the problem into the definitions of ϵ_k and the $V_{a;k}(t)$. The sum over k runs from 0 to ∞; this is true for all the sums over k that appear in the Hamiltonian (1).

The third term describes the interaction between the atomic states and the levels of the metal, where the quantities $V_{a;k}^{(1)}(t)$ and $V_{a;k}^{(2)}(t)$, respectively, describe the coupling of the metal level denoted by k to the atomic state a and to the negative ion state formed by doubly occupying a. Much of the interesting physics of this model originates from this term because it allows electrons to make transitions between the atom and the metal.

The fourth (fifth) term describes the intra-atomic Coulomb repulsion between electrons of different spin which are in different (the same) spatial orbitals. The quantity U_{ab} is the energy cost for forming the negative ion by placing one electron in the atomic state a and placing another electron in the atomic state b; U_{aa} is similarly defined.

To obtain a solution to the Schrödinger equation, the true wave function is approximated by a superposition of a finite number of basis states, each of which is characterized by a specific number of electron-hole pairs.[65] By substituting the approximate wave function into the Schrödinger equation, one can derive equations of motion for the amplitudes of these basis states; these equations can be solved and the amplitudes obtained as a function of time. The square of each amplitude is the occupancy of the corresponding basis state. To obtain the charge state fractions, a sum of the occupancies of the appropriate basis states is calculated (see below). The main approximation in the derivation of the equations of motion is the truncation of the basis set. The truncation may be performed systematically by considering N as a general index and then retaining terms in the equations of motion up to and including those of a particular order in $1/N$.

We define a basis set that includes states which have up to one electron-hole pair, and comment on the implications of this choice of basis. The truncated basis set is given by

$$|a;k\rangle\equiv\left(\frac{1}{N}\right)^{1/2}\sum_\alpha c_a^{\dagger>\alpha}c_{k\alpha}|0\rangle \quad k<k_F, \tag{2}$$

$$|l;k\rangle\equiv\left(\frac{1}{N}\right)^{1/2}\sum_\alpha c_l^{\dagger\alpha}c_{k\alpha}|0\rangle \quad l>k_F, k\leqslant k_F, \tag{3}$$

$$|aa;kq\rangle\equiv\left(\frac{1}{N(N-1)}\right)^{1/2}\sum_{\alpha,\beta} c_a^{\dagger\alpha}c_{k\alpha}c_a^{\dagger\beta}c_{q\beta}|0\rangle \quad q<k\leqslant k_F, \tag{4}$$

$$|aa;kk\rangle\equiv\left(\frac{1}{2N(N-1)}\right)^{1/2}\sum_{\alpha,\beta} c_a^{\dagger\alpha}c_{k\alpha}c_a^{\dagger\beta}c_{k\beta}|0\rangle \quad k\leqslant k_F. \tag{5}$$

The basis state $|0\rangle$ represents a positive alkali ion together with the ground-state metal at $T=0$ K. The basis state $|a;k\rangle$ represents the state of the ion-surface system in which an electron is taken from the metal level denoted by k and is placed into the atomic state a. The basis state $|l;k\rangle$ represents the state of the system in which an electron is taken from the metal level denoted by k and is placed into the metal level denoted by l, where $\epsilon_l>\epsilon_F$; i.e., this is the state with one electron-hole pair. The basis state $|aa;kq\rangle$ represents the state of the system in which two electrons, one taken from the metal level denoted by k and one taken from the metal level denoted by q, are placed into the atomic state a; i.e., this is the negative ion state. The restrictions on k and q are to prevent double counting (i.e., $|aa;kq\rangle$ is indistinguishable from $|aa;qk\rangle$). The basis state $|aa;kk\rangle$ is also a negative ion state, but here the two electrons have been taken from the same level k in the metal.

We approximate the true wave function of the system at time t by a superposition of the basis states defined above:

$$|\Psi(t)\rangle = f(t)|0\rangle + \sum_{k\leq k_F} b_{a;k}(t)|a;k\rangle + \sum_{\substack{k\leq k_F \\ l>k_F}} e_{l;k}(t)|l;k\rangle + \sum_{\substack{k\leq k_F \\ q<k}} d_{aa;kq}(t)|aa;kq\rangle + \sum_{k\leq k_F} d_{aa;kk}(t)|aa;kk\rangle . \tag{6}$$

The probability that the ion-surface system will be found in a state such that the atomic state a is occupied is given by

$$P_a = \sum_{k\leq k_F} |b_{a;k}|^2. \tag{7}$$

We call the entire collection of basis states that involve the $\mathrm{Li}^0(2s)$ state the $\mathrm{Li}^0(2s)$ sector. Thus the sum in the preceding equation is performed over all basis states in the $\mathrm{Li}^0(2s)$ sector. Throughout this paper, we will refer to P_a as the occupancy of the atomic state a. Similarly, we define the charge state fractions P^+ and P^- as

$$P^+ = |f(t)|^2 + \sum_{k\leq k_F} |e_{l;k}|^2 \tag{8}$$

and

$$P^- = \sum_{\substack{k\leq k_F \\ q<k}} |d_{aa;kq}|^2 + \sum_{k\leq k_F} |d_{aa;kk}|^2. \tag{9}$$

We emphasize that the present theory takes a conceptually different approach from that taken to analytically solve the single (atomic) state, time-dependent, Anderson-Newns model.[14] In particular, the present solution is written in terms of the wave function of the ion-surface system, $|\Psi(t)\rangle$, rather than the number operator n_a which specifies the occupation of the atomic state.

To briefly summarize, the final atomic state occupancies of the scattered particle are calculated by solving the Schrödinger equation while using a truncated set of basis states. This basis set permits the production of positive ions, ground-state neutral atoms, negative ions, particle-hole pairs, and excited-state neutral atoms. The present theory describes transitions between the atomic states and the levels of the metal. Auger processes were not included in the calculations presented here, and neither are electron-electron interactions within the metal. As with the Anderson-Newns model with a single atomic state, energy can be deposited in the surface in the form of electron-hole pairs, and the trajectory of the ion is described classically. The present model and the Anderson-Newns model for a single state differ by the presence of the Coulomb repulsion, the addition of excited states, and the production of electron-hole pairs.

The truncated basis set used to obtain the results presented here includes states with only one electron-hole pair, and is illustrated in Fig. 4 for the case of lithium. Other states which should be included in the solution to this order (i.e., other states which involved two electron hops) are those corresponding to excited negative ions and to a neutral atom plus one electron-hole pair. We choose not to include excited negative ion states when calculating the charge state fractions because they are higher in energy (at the distance where the charge state is determined). Also, to our knowledge, no calculations exist to provide estimates of the lifetimes of excited negative ion states near a surface. Here we have not included the states corresponding to a neutral atom plus one electron-hole pair, although this has been done very recently.[66]

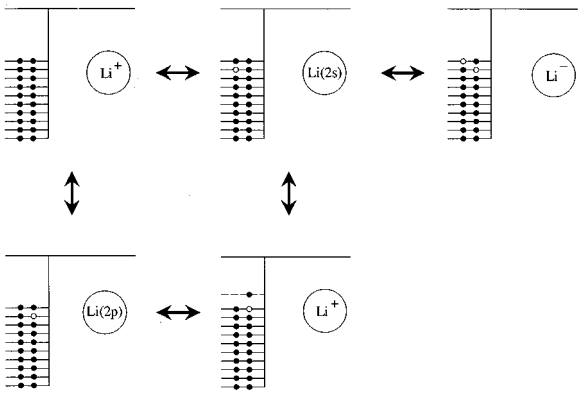

FIG. 4. The restricted basis set employed by Marston *et al.* for Li.

The use of the basis set described above prevents loss of memory of the incident charge state,[7] which has both an experimental and theoretical basis.[9,10,14,20] We correct for this limitation — the truncation of the basis set to states with one electron-hole pair or less — by starting our calculations so that the ion-surface system is in its lowest energy state when the particle is at its distance of closest approach to the surface.[64] This procedure is partly justified because memory loss is accompanied by the attainment of the lowest-energy state of the ion-surface system. We must check, however, that the restriction of the basis set, which prevents memory loss, does not also produce spurious dynamics on the outgoing trajectory. We expect the model to give reliable results if the probability for making one electron-hole pair is small; presumably the probability for making multiple pairs is smaller still. To verify that the probability for making multiple pairs is small requires the inclusion of more basis states. For now, to be consistent, we require the occupancy of the single particle-hole pair sector to be small compared to unity; in practice, we find that the final occupancy of this sector is approximately equal to 0.10 or less.

With the approximations described above, the model can describe the qualitative features of the charge-transfer dynamics if we start the ion-surface system in its lowest-energy state when the ion is at its distance of closest approach to the surface. We therefore started all of the calculations presented in this paper (and the following paper) in this way.

Input to the calculation of the charge state fractions are the energies and lifetimes of the participating atomic levels, the normal velocity of the particle, the density of states of the metal, and the work function of the surface. For the energies of the participating levels, we have used a spline fit to energies calculated by Nordlander,[67] while choosing different saturation values of the level energies near the surface. We plot the calculated energies along with the spline fits in Fig.

TABLE I. Parameters describing the lithium resonance widths calculated by Nordlander, using the three-parameter fit function. In atomic units.

Fit function:
$$\Delta(z)=\exp[a_{-1}/z+\ln\Delta_0-\alpha z]$$

Level	$\ln\Delta_0$	α	a_{-1}
$Li^0(2s)$	2.829	0.9831	−7.776
$Li^0(2p)$	−0.700	0.4691	−1.442
$Li^-(2s^2)$	−2.501	0.3337	−3.057

3. We note here that z is referred to the jellium edge.

The lifetimes of the atomic states are used in the calculations to set the couplings between the states in the metal and the atomic states. We often assume that the lifetimes, and hence the resonance widths, of the states are given by the calculations of Nordlander and Tully[16–18] for $r_s=2.6$ jellium.[67] However, we have also on occasion used the negative ion state resonance width calculated by Teillet-Billy and Gauyacq.[68]

For ease of calculation, we have fit the widths calculated by Nordlander and Tully (or by Teillet-Billy and Gauyacq) with either of two functions. The first function, involving three parameters, is

$$\Delta(z)=\exp[a_{-1}/z+\ln\Delta_0-\alpha z], \tag{10}$$

where $\Delta(z)$ is the half-width at half-maximum of the appropriate resonance. The parameters used to achieve good fits to the calculated values with the function given by Eq. (10) are shown in Table I.

The second function used to fit the calculated widths, which involves four parameters, is

$$\Delta(z)=\frac{\Delta_0}{\left[e^{n\alpha z}+\left(\frac{\Delta_0}{\Delta_{\rm sat}}\right)^n-1\right]^{1/n}}. \tag{11}$$

The parameters used to achieve good fits to the calculated values with the function given in Eq. (11) are shown in Table II.

Comparisons between the lithium level widths calculated by Nordlander and the fit functions are shown in Figs. 5 and 6 for the three- and four-parameter fit functions, respectively.

TABLE II. Parameters describing the lithium resonance widths calculated by Nordlander, using the four-parameter fit function, with $n=4$. In atomic units.

Fit function:
$$\Delta(z)=\frac{\Delta_0}{\left[e^{n\alpha z}+\left(\frac{\Delta_0}{\Delta_{\rm sat}}\right)^n-1\right]^{1/n}}$$
$n=4$

Level	Δ_0	α	$\Delta_{\rm sat}$
$Li^0(2s)$	1.777	0.8290	0.074
$Li^0(2p)$	0.5004	0.5063	0.074
$Li^-(2s^2)$	0.1750	0.3753	0.074

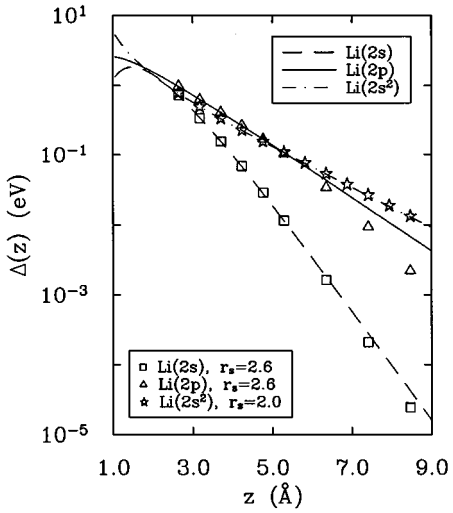

FIG. 5. Comparison of calculated lithium resonance widths and corresponding three-parameter fit functions given by Eq. (10).

The fit functions differ from the calculated widths only at distances for which charge transfer has essentially ceased for the relevant level. For the four-parameter functions, we have simply chosen the saturation values of the resonance widths; we comment on the effects of changing the magnitude of the resonance widths below. We chose the functional forms in Eqs. (10) and (11) since they display an exponential dependence on z far from the surface and have relatively few parameters.

The couplings V, which are the quantities appearing in the many-body Hamiltonian,[7] are obtained from the single-particle relations

$$V^{(1)}_{0;k}(z)=\left(\frac{2\Delta_{2s}(z)}{\pi(NL/D)}\right)^{1/2}, \tag{12}$$

$$V^{(1)}_{1;k}(z)=\left(\frac{2\Delta_{2p_z}(z)}{\pi(NL/D)}\right)^{1/2}, \tag{13}$$

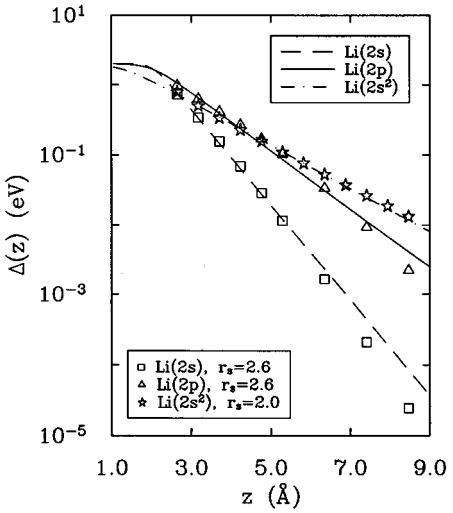

FIG. 6. Comparison of calculated lithium resonance widths and corresponding four-parameter fit functions given by Eq. (11).

$$V_{0;k}^{(2)}(z)=\left(\frac{2\Delta_{2s^2}(z)}{\pi(NL/D)}\right)^{1/2}, \tag{14}$$

where N is the spin degeneracy, L is the number of energy levels between the Fermi level and the bottom of the occupied portion of the metal band, and D is the energy width of the occupied portion of the metal band. Thus NL/D is the density of states of the metal. It is important to note that by specifying the couplings using Eq. (12)–(14), we are assuming the wide-band limit; i.e., the coupling to any state in the metal is the same, independent of the position of the state in the band. Note that the above relations are based on Fermi's golden rule, and are valid only within a single-particle picture; they do not apply in the many-body theory. Because of the ambiguity of obtaining the many-body couplings from atomic state lifetimes derived in a single-particle picture, we feel free to consider the level widths as parameters which can be varied to obtain better agreement with the data.

The normal velocity v_z of the particle during the outgoing trajectory is assumed to be constant. This assumption is expected to be reasonable because classical ion trajectories calculated using the computer code SAFARI (Ref. 69) show that the velocity is rapidly changing only very near the surface. To check if this assumption affects the calculated charge state fractions, we used SAFARI trajectories as input to the calculations. When starting the calculations with the particle at its distance of closest approach and with the ion-surface system in its lowest energy state, we found no difference between the final occupancies obtained using the SAFARI trajectory or the trajectory in which the normal velcocity is assumed to constant. We therefore used constant velocity trajectories for all of the charge-transfer calculations presented in this paper with $v_z=0.02$ a.u. We typically start the particle at $z=1$ Å; we find that the final charge state fractions change by less than 0.02 (absolute) if we start the calculation at $z=2$ Å for work function values $1.29<\phi<4.59$ eV when using the resonance widths given by Eq. (11).

The density of states of the metal is assumed to be constant. The number of metal states used was typically $L=100$ (above and below the Fermi level), with a half-bandwidth $D=4$ eV. This number of metal states was chosen to ensure that the density of states did not affect the results while allowing the calculations to achieve completion in a timely manner. This was done by increasing L and checking how the final charge state occupancies changed. We chose $L=100$ since the final charge state occupancies do not change by more than 0.5% when adding more states.

The metal is described solely by its work-function value, and so an implicit assumption is made that the electrostatic potential outside the surface does not depend on the position *along* the surface. Thus the present version of the theory does not include the effect of the local electrostatic potential. We believe that the present omission of this effect contributes to the discrepancy between the calculations and the data as shown in Sec. V.

V. DISCUSSION

Before we compare the results of the model to the data in detail, it is useful to state a few common results that we recognized after the examination of a large number of calculations. First, the wave function, or initial state, of the ion-surface system when the ion is close to the surface (recall that we have started every calculation presented in this paper with the atom close to the surface) plays a large role in determining the final occupancies. That is, the evolution of the occupancies will depend on the energetics close to the surface and also on the couplings between the basis states which compose the many-body wave function of the system.[71] It is very important to recognize that the energetics change as the surface work function is decreased; this, in turn, changes the initial state, and hence the dynamics, which depend on the instantaneous amplitudes of the different basis states.

Second, the energy differences between the atomic states and the Fermi level of the metal are very important in determining the charge transfer. This is reflected in our finding that it is often true that a significant amount of charge is exchanged between the metal and an atomic state roughly when the atomic state becomes degenerate with the Fermi level. This is due to the fact that, when it becomes energetically favorable during the outgoing trajectory to transfer charge (i.e., when the atomic state and the Fermi level are nearly degenerate), the resonance width of the atomic state (and the associated transition rate) is larger than it is at any other subsequent part of the trajectory.

Third, the relationship between the time scales set by the resonance widths (i.e., the many-body couplings) and the velocity of the scattered particle partly determines the amount of charge transferred during a scattering event. It is necessary to keep *all three* of the above results in mind when explaining the trends in the measured branching ratios; each trend must be individually considered because of the complexity of this system.

Since the initial state of the ion-surface system plays a large role in determining the final charge state fractions, we now discuss it in more detail. We point out that when using the four-parameter function [see Eq. (11)] to fit the resonance widths, all of the resonance widths are the same when $z=1$ Å, i.e., all of the many-body couplings between the basis states are the same. Knowing this, and recalling how the basis states are coupled together (see Fig. 4), one can qualitatively understand why the initial charge state fractions change with work function as shown in Fig. 7. The fact that the couplings at $z=1$ Å are quite large leads to an initial state which is a hybrid of the different basis states, and the degree of hybridization increases as the couplings increase.

The manner in which the basis states are coupled together via the metal surface can lead to initial occupancies which may be nonintuitive. For example, consider the clean surface (i.e., $\phi=4.59$ eV or $\Delta\phi=0.00$ eV): at $z=1$ Å, the $\mathrm{Li}^0(2p)$ state is of higher energy than the $\mathrm{Li}^-(2s^2)$ state (see Fig. 3), yet the initial occupancy of $\mathrm{Li}^0(2p)$ is larger than that of $\mathrm{Li}^-(2s^2)$. This is because the basis states composing the $\mathrm{Li}^0(2p)$ sector are directly coupled to the lowest-energy basis state (for the clean surface, at $z=1$ Å, this is the positive ion basis state with no electron-hole pairs) rather than coupled through an intermediate sector, as is the $\mathrm{Li}^-(2s^2)$ sector (see Fig. 4). [The $\mathrm{Li}^-(2s^2)$ sector is coupled to the positive ion basis state through the $\mathrm{Li}^0(2s)$ sector.] That is, only one electron hop is required for the positive ion to be neutralized into the $\mathrm{Li}^0(2p)$ state while two electron

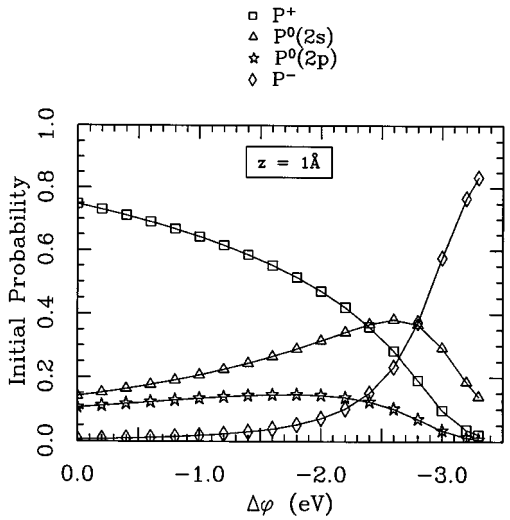

FIG. 7. Calculated initial charge state fractions, at $z=1$ Å, vs the work-function change $\Delta\phi$, using the four-parameter functions [see Eq. (11)] to fit the resonance widths calculated by Nordlander. As $\Delta\phi$ decreases (moving to the right on the $\Delta\phi$ axis), the work function decreases.

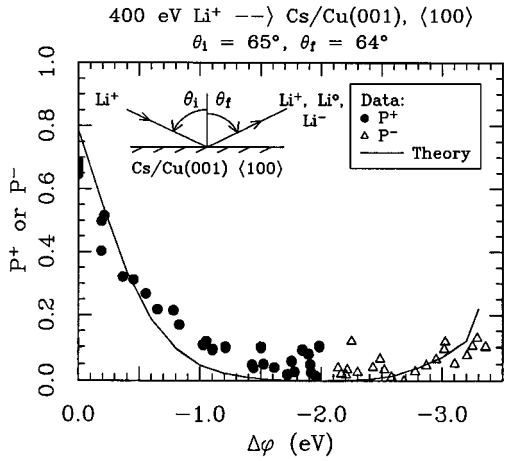

FIG. 8. Comparison of calculated to measured charge state fractions. The fractions were calculated using the four-parameter function [see Eq. (11)] to fit the resonance widths calculated by Nordlander.

hops are required to form the ground-state negative ion. When the work function is decreased, the energy of the positive ion state is effectively increased, while that of the $Li^-(2s^2)$ state decreases, with the result that the $Li^-(2s^2)$ becomes the lowest-energy basis state. This is why the initial occupancy of $Li^-(2s^2)$ rises as the work function decreases. This also explains why the $Li^0(2p)$ state has a very low initial occupancy when the work function is low: it is coupled to the lowest-energy basis state [the $Li^-(2s^2)$ state] only via two intermediate states [i.e., the $Li^0(2s)$ state and either the Li^+ plus one electron-hole pair state or the Li^+ state with no electron-hole pair].

Since the large couplings among the basis states lead to a highly hybridized initial state close to the surface, we see that even basis states that are not energetically favored will have some occupancy when the system is put into its initial state at the beginning of each calculation. As the system evolves in time and the particle moves away from the surface, the energetics and the couplings change, which will change the adiabatic state of the system at every value of z. It is important to remember that the system tries to reach the lowest-energy state in the course of its evolution, and that the ground state far from the surface is the lowest-energy basis state, i.e., the $Li^0(2s)$ state. That the system does not completely evolve into this state indicates that we must concern ourselves with the dynamics, which depend not only on the initial-state occupancies, but on the locations of the Fermi-level crossings for the different atomic states, and on the time scales set by the particle velocity and the couplings between the basis states.

A. Overview

In Fig. 8, we compare calculated charge state fractions to the measured charge state fractions from Fig. 2. The calculated fractions were obtained by using the four-parameter function [see Eq. (11) and Fig. 6]. The model qualitatively reproduces the trends in the data: the decrease in P^+ as the work function is decreased, and the eventual increase of P^-. This behavior is what we expected on the basis of the one-electron picture.[5,58,59,70,42] Here the final charge state fractions reflect changes in the initial state of the ion-surface system; as the work function decreases, the initial occupancies of the $Li^0(2s)$ state and the $Li^-(2s^2)$ state increase (see Fig. 7), as do the corresponding final occupancies. The final charge state fractions also reflect changes in the Fermi-level crossings of the different states. Although similar results have been produced before by the single state Anderson-Newns model[40] (by changing the state involved in the charge transfer for different ranges of work-function values), one should note that the single state Anderson-Newns model was never intended to be applied in cases where substantial neutralization occurs.[14] In contrast, the Coulomb repulsion necessary to describe situations with significant neutralization is included in the present model, along with the different charge states. That the present model correctly obtains the behavior of *both* P^+ and P^- in situations with substantial neutralization and without changing the states involved in the calculation therefore represents a significant advance beyond the single-state Anderson-Newns model. Similar results have been obtained with other models.[34,35,72] The quantitative agreement between the calculation and the data is fortuitous, since the precise values of the calculated charge state fractions, especially P^-, can vary substantially upon changing certain of the input parameters to the calculation by moderate amounts, as we will discuss further in Sec. V B. We also note that the calculation does not reproduce the slope of the experimental curve for P^+. We believe that this is due to the effect of variations in the local electrostatic potential induced by the alkali adsorbates, which we discuss in Sec. VI.

We have investigated the dependence of the calculated charge state fractions on a number of different quantities, such as the magnitude of the resonance widths, the relative magnitudes of the resonance widths, and the initial occupancies of the different basis states. We found that the qualitative trends in the calculated charge state fractions shown in

Fig. 8 are robust if these quantities are varied within reasonable limits, which we describe in Sec. V B.

The calculated charge state fractions follow a few trends, which we note here. First, increasing or decreasing the magnitude of all of the resonance widths by a factor of 2 changes P^+ by only a few percent (absolute) while respectively decreasing or increasing P^- by approximately a factor of 2. Second, increasing only the negative ion state resonance width affects *both* P^+ and P^-, which shows that the negative ion state resonance width affects the dynamics even when the negative ion state is not present in the scattered flux. Third, changing the magnitude and the distance dependence of the resonance widths near the surface ($z<4$ Å) can strongly influence the dynamics of the charge transfer since this changes both the initial state and the relative transition rates between the basis states in the spatial region where all of the rates are relatively large. Fourth, we find that most of the charge transferred comes from states of the metal near the Fermi level, and that significant changes in the atomic state occupancies often occur in the vicinity of the Fermi-level crossing of an atomic state. In fact, as the velocity decreases, the *rate* at which charge is transferred from a particular state of the metal to an atomic state achieves its maximum closer to the value of z for which the state of the metal and the atomic state are degenerate. We also find that, for high work-function values, most of the charge transfer occurs by the time that the atom is about 5 Å from the surface. For low work functions, appreciable charge transfer occurs as far as 10 Å from the surface, primarily because the resonance width associated with the negative ion state (which has a significant final occupancy at low work functions) decays relatively slowly with distance from the surface. We will provide a detailed discussion of these trends in Sec. V B.

B. Details of the dynamics: charge state fractions

To begin this subsection, we investigate how the predicted charge state fractions change as we vary the resonance widths that are used to describe the lifetimes of the various states in the vicinity of the surface. In Fig. 9, we compare the calculated fractions presented in Fig. 8 (obtained using the four-parameter function; see Fig. 6) to those obtained by using the three-parameter function (see Fig. 5) to fit the resonance widths calculated by Nordlander. Recall that the four-parameter function achieves a saturation value at the surface while the three-parameter function does not. Although the predicted values of P^+ are very similar for both fit functions, we find that P^- is more than a factor of 2 larger at the lowest work functions when using the three-parameter function.

The increase in P^- can be explained as follows. The two different sets of width functions lead to initial states of the system which are quite different from one another, as can be seen in the evolutions of the atomic state occupancies shown in Fig. 10 for $\phi=1.29$ eV ($\Delta\phi=-3.30$ eV). This greatly changes the dynamics near the surface (1 Å $<z<$ 4 Å) and consequently alters the charge transfer that occurs between $z=4$ Å and $z=9$ Å. Note that the fits for $Li^-(2s^2)$ state resonance width using the three- and four-parameter functions are very similar except for $z<2$ Å (see Figs. 5 and 6, respectively). Also, the fits for the $Li^0(2s)$ resonance width

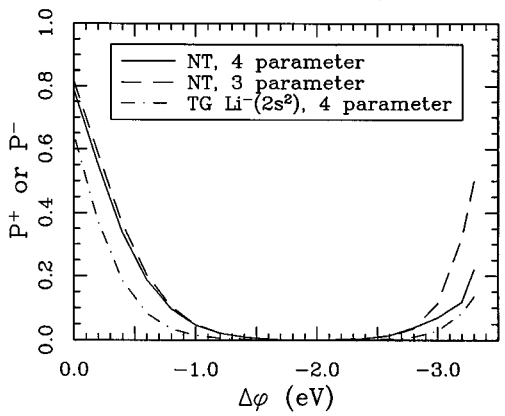

FIG. 9. Comparison of calculated charge state fractions using different resonance widths. See text for description.

are similar except for $z<2$ Å and $z>6$ Å. Given the similarity of the fits over a large region, we see that the dynamics can be strongly influenced by the initial state of the system, which is partly set by the resonance widths of the atomic states.

In Fig. 9, we also show the results obtained by using the negative ion state resonance width calculated by TG, which is fit using the four-parameter function. We note that the resonance width calculated by Teillet-Billy and Gauyacq (TG) is about one-third larger than that calculated by Nordlander (TG include the effect of the polarization of the atom

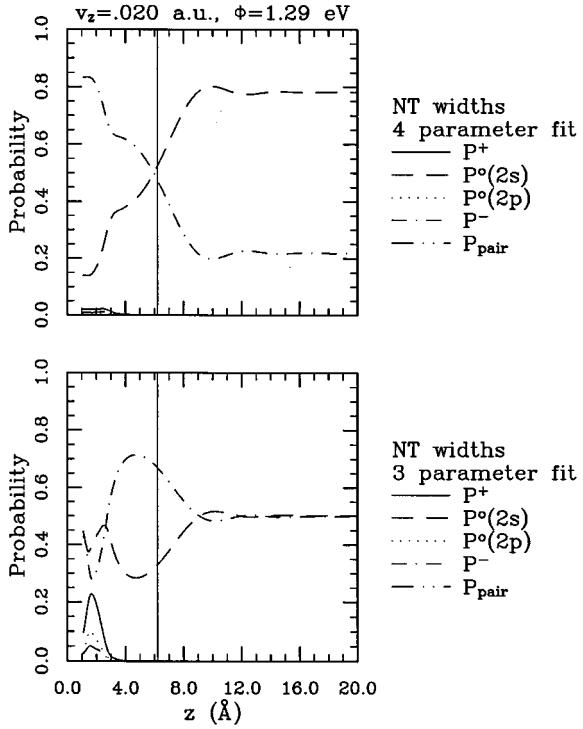

FIG. 10. Evolution of the calculated Li charge state occupancies, for $v_z=0.02$ a.u. and $\phi=1.29$ eV ($\Delta\Phi=-3.30$ eV). (a) Using the four-parameter function to fit the Nordlander resonance widths. (b) Using the three-parameter function [see Eq. 10)] to fit the Nordlander resonance widths. The vertical lines indicate the Fermi level crossing distance for the effective affinity level.

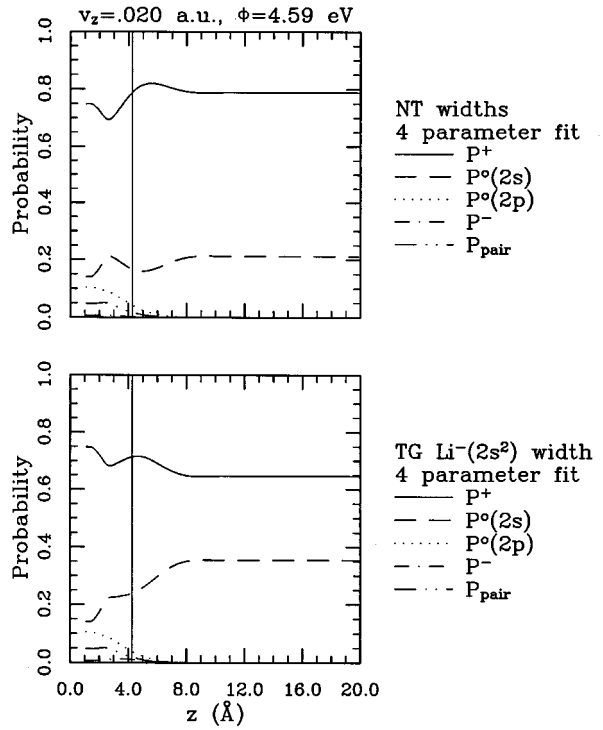

FIG. 11. Evolution of the calculated Li charge state occupancies, for $v_z=0.02$ a.u. and $\phi=4.59$ eV ($\Delta\phi=0.00$ eV). (a) Using the four-parameter function to fit the Nordlander resonance widths. (b) Using the four-parameter function to fit the TG resonance width. The vertical lines indicate the Fermi level crossing distance for the effective ionization level.

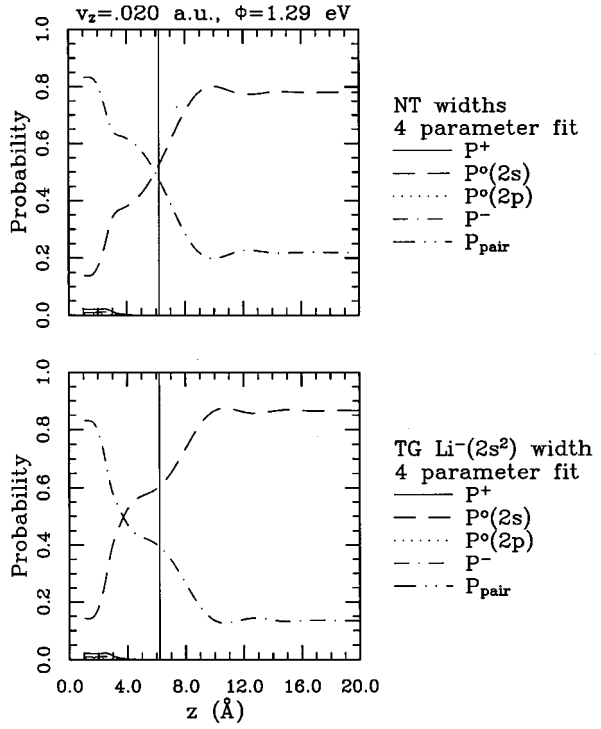

FIG. 12. Evolution of the calculated Li charge state occupancies, for $v_z=0.02$ a.u. and $\phi=1.29$ eV ($\Delta\phi=-3.30$ eV). (a) Using the four-parameter function to fit the Nordlander resonance widths. (b) Using the four-parameter function to fit the TG resonance width. The vertical lines indicate the Fermi level crossing distance for the effective affinity level.

by the surface potential[73]). One can see that, for a given work function, using the negative ion state resonance width calculated by TG decreases P^+, and slightly decreases P^- with respect to using the negative ion state resonance width calculated by Nordlander.

The decrease in P^+ obtained when using the negative ion state resonance width of TG can be explained as follows. The larger negative ion state resonance width calculated by TG gives a larger coupling between the $Li^-(2s^2)$ state, and the metal appears to hinder the transfer of electrons from the $Li^0(2s)$ state to the metal in the region 2.5 Å$<z<$6.0 Å. This can be seen by examining the evolutions of the occupancies obtained using the Nordlander and TG negative ion state resonance widths. These are shown for $\phi=4.59$ eV ($\Delta\phi=0.00$ eV) in Fig. 11. There it is shown that the initial states of the system are identical (because the saturation values of the level widths are chosen to be the same for both the Nordlander and TG negative ion state resonance widths), and that the main differences in the evolutions occur between $z=3$ Å and 8 Å. When using the Nordlander width for the negative ion state, P^+ increases by about 0.14 between $z=2.5$ and 6.0 Å [recall that the $Li^0(2s)$ state crosses the Fermi level near 4.3 Å, and that the system does not respond instantaneously to crossing the Fermi level]. However, when using the TG result for the negative ion state resonance width, P^+ increases by only 0.05 in the same z interval, which demonstrates that the transfer of the electron from the $Li^0(2s)$ state to the metal is less efficient. The occupancy of the $Li^-(2s^2)$ state is hardly changed at $z=1$ Å when using the TG resonance width (0.0066 compared to 0.0065 with the Nordlander resonance width), yet changing the distance dependence of the $Li^-(2s^2)$ resonance width produces a significant change in the final occupancies of the other channels.

The larger negative ion state resonance width of TG leads to a slightly decreased P^- (Fig. 9) because it increases the rate at which electrons can hop between the negative ion and the metal, thereby increasing the rate of $Li^0(2s)$ production when the $Li^0(2s)$ state is energetically favored. This is most evident for 2 Å$<z<$4 Å in Fig. 12, which shows the evolutions of the occupancies for $\phi=1.29$ eV ($\Delta\phi=-3.30$ eV). The first sharp decrease of P^- begins when the $Li^0(2s)$ state becomes more energetically favorable than the $Li^-(2s^2)$ state ($z\approx1.7$ Å); the second sharp decrease occurs approximately where the $Li^-(2s^2)$ state crosses the Fermi level (at $z\approx6.2$ Å).

By using different resonance widths for the negative ion state, we have shown that the charge state fractions are affected even when the negative ion state is not present in the scattered flux, which illustrates the importance of including multiple states in the theoretical description of charge transfer. That the intra-atomic correlation must be included to obtain qualitatively correct results has been demonstrated previously by Langreth and Nordlander.[37] These results also demonstrate that the time scales set by the resonance widths affect the charge transfer.

To test the sensitivity of the charge state fractions to changing all of the resonance widths, we compare the results

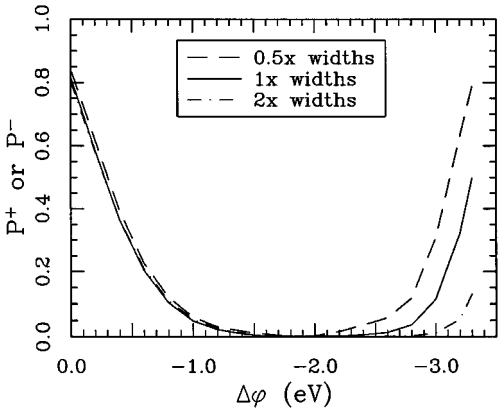

FIG. 13. Comparison of charge state fractions calculated with different resonance widths. For $v_z = 0.02$ a.u. See text for description.

obtained with the resonance widths calculated by Nordlander to results obtained by doubling and halving the same resonance widths, as shown in Fig. 13. Here the three-parameter functions are used to fit the calculated resonance widths. We see that, for a given work function, the values of P^+ obtained are very similar, but that the values of P^- differ markedly from one another. At low work functions, P^- decreases when the resonance widths are all increased by the same factor. It is important to recognize that although there are quantitative differences between the charge state fractions calculated using the different resonance widths, the basic trends remain the same.

To explain the differences between the predicted values of P^- shown in Fig. 13, we examine the evolutions of the occupancies for $\phi = 1.29$ eV ($\Delta\phi = -3.30$ eV) in Fig. 14. We find that changing all the resonance widths by a constant factor produces quite different initial states of the ion-surface system. We also find that the larger the transition rate is near the Fermi-level crossing, the larger the decrease is in the occupancy of $\mathrm{Li}^-(2s^2)$, as can be seen by comparing Figs. 14(a)–14(c) in the region 4 Å$< z <$8 Å. Thus a combination of different initial occupancies and different transition rates (i.e., time scales) in the vicinity of the Fermi level crossing leads to the large differences in P^-.

We explain the fact that changing all of the resonance widths by the same factor causes only small changes in P^+ for high work functions by noting two competing trends which can be seen in Fig. 15. First, the larger the $\mathrm{Li}^0(2s)$ resonance width, the more that the $\mathrm{Li}^0(2s)$ resonance lies below the Fermi level, and hence the larger the occupancy of the $\mathrm{Li}^0(2s)$ state. [In Fig. 15, the changes are modest: $P^0(2s)$, for example, increases by about 0.05 when doubling all of the resonance widths.] Second, the larger the $\mathrm{Li}^0(2s)$ resonance width, the more charge is transferred back to the metal as the particle moves from $z = 3$ to 5 Å, i.e., the more the occupancy of the $\mathrm{Li}^0(2s)$ state decreases. These two trends compete with one another, and the net effect is that P^+ changes only a little as the resonance widths are changed. This is in contrast to what is found in the single state Anderson-Newns model,[20] where changing the lifetime by a factor of two leads to changes in P^+ that are approximately twice as large as in the present model.

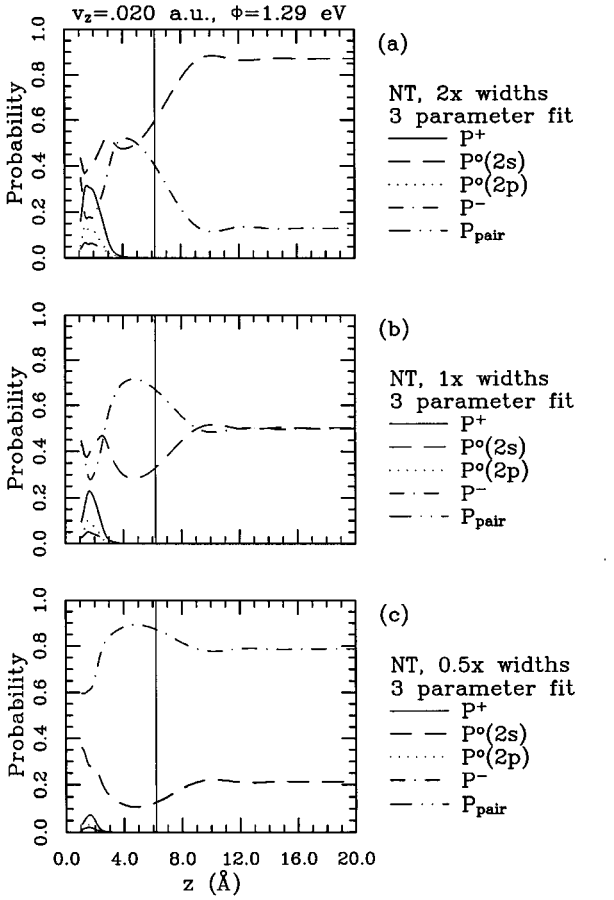

FIG. 14. Evolution of the calculated Li charge state occupancies, for $v_z = 0.02$ a.u. and $\phi = 1.29$ eV ($\Delta\phi = -3.30$ eV). (a) Using $2\times$ the three-parameter function to fit the Nordlander resonance widths. (b) Using the three-parameter function to fit the Nordlander resonance widths. (c) Using $0.5\times$ the three-parameter function to fit the Nordlander resonance widths. The vertical lines indicate the Fermi-level crossing for the effective affinity level.

VI. EFFECT OF THE LOCAL ELECTROSTATIC POTENTIAL

We noted in Sec. V that the work-function dependence of the measured charge state fractions has a smaller (absolute value of the) slope than that predicted by the theoretical model [this is also the case for the relative $\mathrm{Li}^0(2p)$ yields, as shall be seen in paper II]. We must therefore investigate possible explanations for the discrepancy between the predicted and the observed work function dependence of the charge state fractions and the relative $\mathrm{Li}^0(2p)$ yields.

One possibility, suggested by previous work,[14,24,29,30,38,42–46,53] is that the local adsorbate-induced electrostatic potential surface broadens the work-function dependence. In the experiments described in this paper, the work function is lowered by depositing varying amounts of alkali atoms onto the Cu(001) surface. Upon adsorption, the alkalis behave like dipoles on the surface, and modify the local electrostatic potential accordingly. Since our experiments are performed in the regime of low coverages, the adsorbate spacing is always approximately two lattice constants (≈ 7 Å) or greater, and the local electrostatic potential varies *along* the surface. How the potential varies along the

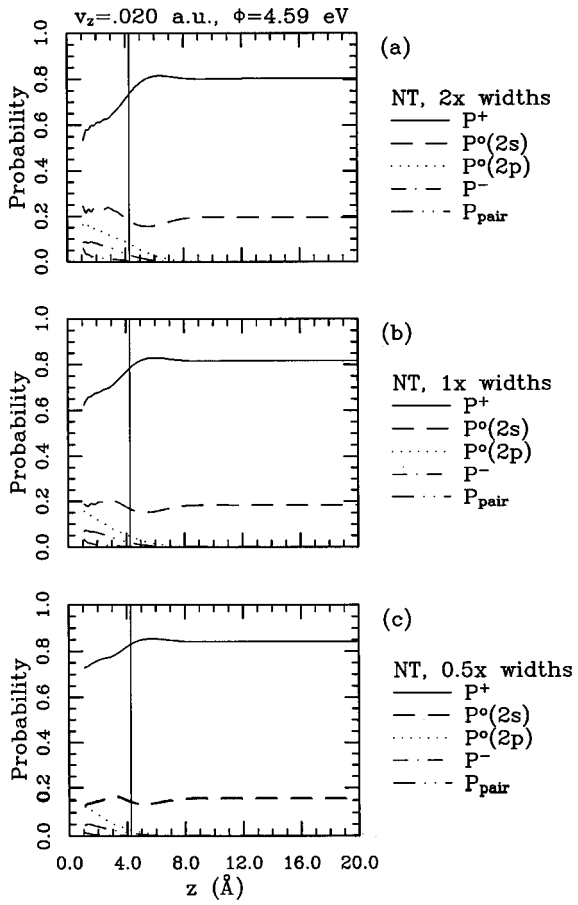

FIG. 15. Evolution of the calculated Li charge state occupancies, for $v_z = 0.02$ a.u., and $\phi = 4.59$ eV ($\Delta\phi = 0.00$ eV). (a) Using $2\times$ the three-parameter function to fit the Nordlander resonance widths. (b) Using the three-parameter function to fit the Nordlander resonance widths. (c) Using $0.5\times$ the three-parameter function to fit the Nordlander resonance widths. The vertical lines indicate the Fermi level crossing for the effective ionization level.

surface is not known, and certainly changes with coverage. Since the energies of the atomic levels participating in the charge transfer are affected by the local electrostatic potential,[48,49] the energy of the level varies as the particle moves along the surface (i.e., closer to or farther from adsorbate atoms).[74]

For the experiments described here, the scattering particle samples many different local electrostatic potentials instead of one, as we assumed in applying the theory of Marston *et al.* When the inhomogeneous potential is included, the result is a broadening of the theoretical curves of $Li^0(2s)$ formation probability versus $\Delta\phi$ (i.e., coverage). This has been shown in the work of Geerlings, Kwakman, and Los[40] and Kimmel and co-workers,[41,42] who included the local electrostatic potential in the single state Brako-Newns model. Of particular relevance here is the recent work by Weare and Yarmoff,[46] which showed the same broadening, but using the model of Marston *et al.* In particular, they compared calculations with and without including inhomogeneities to measurements of charge state fractions for Li undergoing a single collision with either an alkali adsorbate or a substrate atom on alkali-covered Al(100). Incorporation of the local electrostatic potential as in the works above effectively results in the spatial averaging of that potential. On the basis of these and other works, we expect that the effect of the local adsorbate-induced electrostatic potential is the main reason why the measured formation probabilities vary more slowly with work-function change than the present theory would predict. Nonetheless, the qualitative dependences of the probabilities with and without the inhomogeneous potential are the same, and the quantitative differences are small, so we expect that the dynamics of charge transfer are not qualitatively changed by including the inhomogeneous potential.[75]

We note that a different explanation for the observed broadening of the work-function dependence of the charge state fractions has been given. Zimny presented a theoretical study in which the broadening of the charge-transfer data of Geerlings *et al.* can be explained by including the effect of spin[23] and the effect of the parallel velocity of the ion on the apparent energies of the metal electrons. This model, which is based on a rate-equation approach, does not include the effect of the local electrostatic potential. This model was also used to describe measurements, performed by by Jiang, Li, and Koel, of the relative ion yields that result when Li^+ ions scatter from Cs adsorbates on a Ni(111) surface for different Cs coverages.[76] Although glancing angles are required for the application of the Zimny model ($\theta_f \geqslant 80°$), Jiang, Li, and Koel found that the relative yields measured at a glancing final angle ($\theta_f = 70°$) could be reproduced well by the model of Zimny. Jiang, Li, and Koel also found that it was important to include spin properly. We note that our measurements were conducted at $\theta_f = 64°$, and that the inclusion of spin in the model of Marston *et al.* does not broaden the work function dependence enough to fit the data (see Fig. 8). Finally, the Zimny model does not include excited states or negative ions. Its range of applicability is therefore not sufficient to describe our entire set of data (which includes data in paper II).

Finally, we note that it has been suggested that the inclusion of the local electrostatic potential in a semiclassical model based on the single-state Brako-Newns model cannot account for the observed broadening of the work-function dependence of the charge state fractions. Ashwin and Woodruff measured the relative yields of scattered Li^+ ions that result when scattering 1-keV Li^+ from Cs/Cu(110) with an incident angle of $\theta_i = 13°$ and a final angle of $\theta_f = 17°$.[77] Their observations of Li^+ scattered from Cs adsorbates cannot be reconciled with a single-state semiclassical model modified to include the adsorbate-induced potential.[24] Such a model predicts a unit neutralization probability for scattering from a Cs adsorbate. Thus the observation of positive ions scattered directly from Cs adsorbates indicate that the single-state model is incomplete. However, these observations do not rule out the hypothesis that the local adsorbate-induced potential can account for the observed broadening of the work function dependence of the charge state fractions. For the incident beam energies utilized by Ashwin and Woodruff, autoionization processes, typically omitted by most charge-transfer models, can occur.[78,79] These processes may be responsible for the ions that they observe.

To summarize, a large body of evidence has accumulated which supports the idea that the electrostatic potential in the vicinity of alkali adsorbates varies significantly with regard

to charge transfer. We expect that it is important to include such variations in the potential to obtain quantitative agreement with the measured work-function dependence of the charge state fractions and excited-state yields.

VII. SUMMARY

In this paper, we presented measurements of the charge state fractions in the flux scattered into $\theta_f = 64°$ that result when Li^+ ions impinge on Cs/Cu(001) with energy $E_i = 400$ eV, an incident angle $\theta_i = 65°$, and along the $\langle 100 \rangle$ azimuth. As the work function of the surface decreases, the fraction of particles scattered as positive ions monotonically decreases and eventually the fraction of particles scattered as negative ions increases.

We have seen that the many-body theory of Marston *et al.* reproduces the trends seen in the observed charge state fractions. Although the production of electron-hole pairs was limited to one by the practical implementation of the theory,[66] which prevents complete loss of memory of the incident charge state, the model can be applied to describe the data when the model system is started in its lowest-energy state when the ion is close to the surface.

By performing theoretical calculations for a range of input parameters, we found that the state of the system when the ion is at its distance of closest approach to the surface strongly influences the charge transfer, that there is often a significant amount of charge transferred in the vicinity of the relevant Fermi level crossings, and that the changing relationships between the time scales set by the velocity of the scattering particle and the transition rate set by the resonance widths of the relevant atomic states also play a role in determining the charge transfer. We suggest that the differences between the measured and predicted fractions are at least partially due to the effect of the adsorbate-induced local electrostatic potential. The results presented here show that the measured charge state fractions can be accounted for by assuming that the resonant charge-transfer mechanism governs the evolution of the ion-surface system during the outgoing trajectory of the scattering particle.

Note added in proof. Recent work by Borisov *et al.* indicates that the resonance broadening and level energy can be quite different for collisions with adsorbate atoms and substrate atoms. Most of the collisions in our experiments take place with the substrate and not on top of an adsorbate. Calculations are not yet available to include the adsorbate effects in an averaged way. To achieve quantitative agreement with experiment, such calculations will have to be done.

ACKNOWLEDGMENTS

We thank Eric Dahl, David Goodstein, and Craig Keller for many useful discussions. We also thank Peter Nordlander, Jean-Pierre Gauyacq, and Dominique Teillet-Billy for giving us the results of their lifetime calculations for use in this study. This research was funded by the Air Force Office of Scientific Research (AFOSR-91-0137), by the National Science Foundation (NSF-DMR-9022961), and the Cornell Materials Science Center (NSF-DMR-9121654). D.R.A. was also supported by the Swedish Institute and the Sweden-America Foundation. J.B.M. was partially supported by the National Science Foundation (NSF-DMR-9357613).

*Present address: The Department of Physics and Astronomy, 303 Strong Hall, Eastern Michigan University, Ypsilanti, MI 48197.
†Present address: Department of Applied Physics, Chalmers University of Technology, S-41296 Göteborg, Sweden.

[1] J. J. C. Geerlings and J. Los, Phys. Rep. **190**, 133 (1990).
[2] R. Brako and D. M. Newns, Rep. Prog. Phys. **52**, 655 (1989).
[3] A. T. Amos, K. W. Sulston, and S. G. Davison, in *Advances in Chemical Physics* (Wiley, New York, 1989), Vol. LXXVI, pp. 335–368.
[4] S. R. Kasi, H. Kang, C. S. Sass, and J. W. Rabalais, Surf. Sci. Rep. **10**, 1 (1989).
[5] E. R. Behringer, D. R. Andersson, D. M. Goodstein, B. Kasemo, B. H. Cooper, and J. B. Marston, Nucl. Instrum. Methods Phys. Res. Sect. B **78**, 3 (1993).
[6] D. R. Andersson, E. R. Behringer, B. H. Cooper, and J. B. Marston, J. Vac. Sci. Technol. A **10**, 2196 (1993).
[7] J. B. Marston, D. R. Andersson, E. R. Behringer, C. A. DiRubio, G. A. Kimmel, C. Richardson, and B. H. Cooper, Phys. Rev. B **48**, 7809 (1993).
[8] In principle, these channels can be added but doing so introduces parameters which may not be well known. See, for example, Ref. 66 for very recent work adding the Auger channel.
[9] J. Hermann, B. Welle, J. Gehring, H. Schall, and V. Kempter, Surf. Sci. **138**, 570 (1984).
[10] B. Hird, P. Gauthier, J. Bulicz, and R. A. Armstrong, Phys. Rev. Lett. **67**, 3575 (1991).
[11] A. J. Algra, E. v. Loenen, E. P. Th. Surmeier, and A. L. Boers, Radiat. Eff. **60**, 173 (1982).
[12] P. W. Anderson, Phys. Rev. **124**, 41 (1961).
[13] D. M. Newns, Phys. Rev. **178**, 1123 (1969).
[14] R. Brako and D. M. Newns, Surf. Sci. **108**, 253 (1981).
[15] G. A. Kimmel and B. H. Cooper, Phys. Rev. B **48**, 12 164 (1993).
[16] P. Nordlander and J. C. Tully, Phys. Rev. Lett. **61**, 990 (1988).
[17] P. Nordlander and J. C. Tully, Surf. Sci. **211/212**, 207 (1989).
[18] P. Nordlander and J. C. Tully, Phys. Rev. B **42**, 5564 (1990).
[19] J.N.M. van Wunnik, R. Brako, K. Makoshi and D. M. Newns, Surf. Sci. **126**, 618 (1983).
[20] G.A. Kimmel, Ph.D. Thesis, Cornell University, 1992.
[21] H. Winter and R. Zimny, in *Coherence in Atomic Collision Physics*, edited by H. J. Beyer, K. Blum, and R. Hippler (Plenum, New York, 1988).
[22] R. Zimny, H. Nienhaus, and H. Winter, Radiat. Eff. Defects Solids **109**, 9 (1989).
[23] R. Zimny, Surf. Sci. **233**, 333 (1990).
[24] J. J. C. Geerlings, R. Rodink, J. Los, and J. P. Gauyacq, Surf. Sci. **181**, L177 (1987).
[25] J. J. C. Geerlings, R. Rodink, J. Los, and J. P. Gauyacq, Surf. Sci. **186**, 15 (1987).
[26] H. Schall, W. Huber, H. Hoermann, W. Maus-Friedrichs, and V. Kempter, Surf. Sci. **210**, 163 (1989).
[27] H. Schall, H. Brenten, K. H. Knorr, and V. Kempter, Z. Phys. D **16**, 161 (1990).
[28] H. Brenten, H. Müller, K. H. Knorr, D. Kruse, H. Schall, and V. Kempter, Surf. Sci. **243**, 309 (1991).
[29] J. J. C. Geerlings and J. Los, Phys. Lett. A **102**, 204 (1984).
[30] J. J. C. Geerlings, L. F. Tz. Kwakman, and J. Los, Surf. Sci. **172**, 257 (1987).

[31] T. B. Grimley, V. C. Jyothi Bhasu, and K. L. Sebastian, Surf. Sci. **124**, 305 (1983).
[32] K. L. Sebastian, Phys. Rev. B **31**, 6976 (1985).
[33] H. Kasai and A. Okiji, Surf. Sci. **183**, 147 (1987).
[34] H. Nakanishi, H. Kasai, and A. Okiji, Surf. Sci. **197**, 515 (1988).
[35] K. W. Sulston, A. T. Amos, and S. G. Davison, Phys. Rev. B **37**, 9121 (1988).
[36] K. W. Sulston, A. T. Amos, and S. G. Davison, Surf. Sci. **224**, 543 (1989).
[37] D. C. Langreth and P. Nordlander, Phys. Rev. B **43**, 2541 (1991).
[38] C. C. Hsu, H. Bu, A. Bousetta, J. W. Rabalais, and P. Nordlander, Phys. Rev. Lett. **69**, 188 (1992).
[39] H. Shao, D. C. Langreth, and P. Nordlander, *Low Energy Ion-Surface Interactions*, edited by J. W. Rabalais (Wiley, New York, NY, 1993).
[40] J. J. C. Geerlings, L. F. Tz. Kwakman, and J. Los, Surf. Sci. **184**, 305 (1987).
[41] G. A. Kimmel, D. M. Goodstein, and B. H. Cooper, J. Vac. Sci. Technol. A **7**, 2186 (1989).
[42] G. A. Kimmel, D. M. Goodstein, Z. H. Levine, and B. H. Cooper, Phys. Rev. B **43**, 9403 (1991).
[43] Z. L. Miskovic, S. G. Davison, and F. O. Goodman, Phys. Rev. Lett. **71**, 4075 (1993).
[44] C. B. Weare and J. A. Yarmoff, J. Vac. Sci. Technol. A **13**, 1421 (1995).
[45] C. B. Weare, K. A. H. German, and J. A. Yarmoff, Phys. Rev. B **52**, 2066 (1995).
[46] C. B. Weare and J. A. Yarmoff, Surf. Sci. **348**, 359 (1996).
[47] With certain systems and a high-resolution detection scheme, experiments can be done which do not require averaging theoretical results over different trajectories to make a quantitative comparison between theory and experiment. See, for example, Refs. 44–46. With the Li^+-Cs/Cu(001) system and the detection scheme described in this paper, it is necessary to average theoretical results in order to perform a quantitative comparison with experiment.
[48] P. Nordlander and N. D. Lang, Phys. Rev. B **44**, 13 681 (1991).
[49] A. G. Borisov, G. E. Makhmetov, D. Teillet-Billy, and J. P. Gauyacq, Surf. Sci. **350**, L205 (1996).
[50] R. L. McEachern, D. L. Adler, D. M. Goodstein, G. A. Kimmel, B. R. Litt, D. R. Peale, and B. H. Cooper, Rev. Sci. Instrum. **59**, 2560 (1988).
[51] D. L. Adler and B. H. Cooper, Rev. Sci. Instrum. **59**, 137 (1988).
[52] P. W. van Amersfoort, J. J. C. Geerlings, L. F. Tz. Kwakman, E. H. A. Granneman, and J. Los, J. Appl. Phys. **58**, 2312 (1985).
[53] G. A. Kimmel and B. H. Cooper, Rev. Sci. Instrum. **64**, 672 (1993).
[54] Only a portion of the spectrum is integrated because the low-energy tail of the spectrum contains particles that have gone underneath the first layer, and recent results show that these particles can undergo anomalously high neutralization [see C. A. Keller *et al.*, Phys. Rev. Lett. **75**, 1654 (1995)]. In addition, part of the intensity at long arrival times (low energies) may contain sputtered particles, and it is necessary to exclude these from the calculation of the charge fraction.
[55] SAES Getters/USA Inc., Colorado Springs, CO.
[56] J. Cousty, R. Riwan, and P. Soukiassian, Surf. Sci. **152/153**, 297 (1985).
[57] C. A. Papageorgopoulos, Phys. Rev. B **25**, 3740 (1982).
[58] R. W. Gurney, Phys. Rev. **47**, 479 (1935).
[59] J. W. Gadzuk, Surf. Sci. **6**, 133 (1967).
[60] D. M. Newns, K. Makoshi, R. Brako, and J. N. M. van Wunnik, Phys. Scr. **T6**, 5 (1983).
[61] N. D. Lang, S. Holloway, and J. Nørskov, Surf. Sci. **150**, 24 (1985).
[62] D. M. Goodstein, Ph.D. thesis, Cornell University, 1990.
[63] We are assuming that the atom is a few Å from the surface, since this is where the charge state is determined.
[64] R. Brako and D. M. Newns, Solid State Commun. **55**, 633 (1985).
[65] The technique used to obtain a solution to the Schrödinger equation for the model system described by Eq. (1) is a systematic expansion in particle-hole pairs (here the particles are electrons). The truncation may be performed systematically by retaining terms in the equations of motion up to and including those characterized by a certain number of particle-hole pairs.
[66] A. Onufriev and J. B. Marston, Phys. Rev. B **53**, 13 340 (1996). Onufriev and Marston recently extended the truncated basis set to include the sector with a neutral atom plus a particle-hole pair. The results of their work do not change the conclusions given in the summary of the present paper and show that loss of memory is improved.
[67] P. Nordlander (private communication).
[68] D. Teillet-Billy and J. P. Gauyacq (private communication).
[69] D. M. Goodstein, S. A. Langer, and B. H. Cooper, J. Vac. Sci. Technol. A **6**, 703 (1988).
[70] J. N. M. van Wunnik, R. Brako, K. Makoshi, D. M. Newns, and J. Los, Phys. Scr. **T6**, 27 (1983).
[71] One might wonder if the fact that the evolutions of the occupancies depend on the occupancies at the surface implies that they may also depend on the initial charge state far from the surface (i.e., memory is not lost). This is not so. With a model that achieves memory loss, the state of the ion-surface system when the ion is at its distance of closest approach will be independent of the charge state far from the surface. However, the evolutions of the occupancies during the outgoing trajectory will still depend on the instantaneous occupancies, which in turn depend on the energetics at the distance of closest approach.
[72] B. Hellsing and V. Zhdanov, Surf. Sci. **274**, 411 (1992).
[73] D. Teillet-Billy and J. P. Gauyacq, Surf. Sci. **239**, 343 (1990).
[74] We do not expect the energy of an atomic level to *follow* the local electrostatic potential if the atom and adsorbate are sufficiently close. Another possible effect of the inhomogeneous potential is that the resonance broadening of an atomic level may be different near an adsorbate.
[75] We think that the effective spatial averaging of the inhomogeneous potential, together with the following reasons, support the idea that the charge transfer dynamics described in this paper qualitatively describe those of most of the scattered particles. First, the fraction of particles which scatter directly from an adsorbate is low for low coverages, and so the majority of particles scatter from the substrate. Second, at higher coverages and relatively glancing angles of incidence, where the fraction may be a few tens of percent, the effect of the inhomogeneous potential is experimentally seen to disappear (see Refs. 44–46).
[76] L. Q. Jiang, Y. D. Li, and B. E. Koel, Phys. Rev. Lett. **70**, 2649 (1993).
[77] M. J. Ashwin and D. P. Woodruff, Surf. Sci. **244**, 247 (1991).
[78] K. A. H. German, C. B. Weare, and J. A. Yarmoff, Phys. Rev. Lett. **72**, 3899 (1994).
[79] K. A. H. German, C. B. Weare, and J. A. Yarmoff, Phys. Rev. B **50**, 14 452 (1994).